FIRST QUARTERLY REPORT

RESEARCH AND DEVELOPMENT

IN

CdS PHOTOVOLTAIC FILM CELLS

by

J. C. Schaefer, E. R. Hill, T. A. Griffin

Prepared for

NATIONAL AERONAUTICS AND SPACE ADMINISTRATION

June 28, 1965 to September 28, 1965

Contract NAS 3-7631

Technical Management
NASA Lewis Research Center
Cleveland, Ohio
Space Power Systems Division
Clifford Swartz

Harshaw Chemical Company
Crystal-Solid State Division
1945 E. 97th Street
Cleveland 6, Ohio

FOREWARD

This report was prepared by the Crystal-Solid State Division of the Harshaw Chemical Company. The work has been sponsored by the Space Power Systems Procurement Section of the NASA Lewis Research Center with Dr. A. E. Potter acting as Technical Advisor and Mr. Clifford Swartz acting as Project Manager.

Dr. J. McKenzie is the Technical Director of the Solid State Laboratory of the Harshaw Chemical Company. Project direction has been provided by Mr. J. C. Schaefer with Mr. E. R. Hill, Mr. T. A. Griffin and Mr. R. Rautenstrauch acting as principal investigators for the research development, and pilot line work respectively. The following Harshaw personnel have contributed to this program: B. Keramidas, D. J. Krus, W. W. Baldauf, N. E. Heyerdahl, P. Marn and C. A. Morano. Dr. N. K. Pope of the Royal Military College of Canada served as consultant.

TABLE OF CONTENTS

LIST OF FIGURES

SUMMARY

This program is designed to produce CdS solar cells in accordance with the recently proposed solar cell model. Additional model investigations are reported. Vapor transport procedures have been used to produce improved films of CdS. A large improvement has been made in the procedure for forming collector grids by electroplating. This grid technique provides the highest cell stability during thermal cycling. An interface film of silver between substrate and CdS appears to be beneficial. Single crystal Cu_2S has been grown by vapor transport methods.

INTRODUCTION

The cadmium sulfide (CdS) solar cell in its present state of development is composed of a thin evaporated film of CdS on a conductive substrate with a barrier layer formed along the surface of the film. The substrate also serves as a current collector. A grid is affixed to the barrier layer in order to collect the available power. Since the cell is changing rather often a more specific description is not warranted.

Further changes are dictated by the recent model concept reported at the Photovoltaic Specialist Conference in October at the NASA, Goddard Space Flight Center. Uniform layer thicknesses of CdS and cuprous sulfide (Cu_2S) are desired if a maximum conversion efficiency and power output are to be achieved.

Evaporated CdS films do not provide the desired qualities. Experiments to form films by vapor transport have indicated that the desired film thickness, uniformity, freedom from pin holes and cracks, and control of bulk film properties are possible. The application of a uniformly thick vapor transported barrier layer would provide a cell within the concept of the CdS model. Barrier formation by solution dipping or electroplating fails to produce a uniform thickness or continuity.

This approach may prove to be significant since a low material utilization is inherent in evaporation, whereas, a very high utilization factor is immediately apparent for the vapor transport method. This will be a major consideration in production.

CdS vapor transported films have been made and fabricated into cells with efficiencies up to 3.5%. The barrier material has been prepared as single crystal Cu_2S but not as film.

Current collection at the barrier layer has always been a problem. Good collection of current initially and throughout prolonged thermal cycling are the prime objectives. Operating cells with collector grids applied by electroplating have accomplished the objectives. When the procedure was initially introduced, the yields were very low. Recent improvements have upgraded the yield to nearly 80%. The attack on the cells by the plating solutions has been the greatest problem.

Electrochemical etching of the substrates after fabrication appears to be practical when required.

Several interface coatings have been applied between the substrate and the CdS film. Indications are that silver may be beneficial in reducing contact resistance.

Cell Model and Measurements

The CdS Solar Cell Model leaves some questions unanswered. Additional measurements are necessary to probe further.

Clues to the mechanisms involved in the CdS solar cell can be obtained by a study of the current-voltage data. Generally the device can be described by the diode equation:

$$I = I_o \left(\exp \frac{qV}{KT} - 1\right)$$

with appropriate alowances for series and shunt resistance effects. The term, I_o, is the leakage current, is temperature dependent, determined by the materials on each side of the junction. To explain deviations in the negative voltage region, it is sometimes assumed that I_o is also voltage dependent. In any case, it is clear that this is an equation of state for the device and uniquely determines I at any particular voltage and temperature. The q is the electrical charge, V is the voltage, K is a constant, while T is the temperature in ^oK. However, referring to Figure 1, it can be seen that the I-V curve for a typical CdS cell is not single valued when traced at the rate of 1 cycle in 48 hours. It is important to determine whether this hysteresis exists in the steady state or is simply a long term transient phenomenon. I-V curves have been measured at various frequencies and analyzed. The result of the anlysis has been to show that at frequencies above 10 sec^{-1}, the cell behaves as a normal diode and can be described as a rectifier with a parallel capacitance of 10^{-1} to 10^{-2} microfarads per cm^2. As frequency is decreased, another effect sets in, with the behavior shown in Figure 1. This hysteresis effect increases as the frequency decreases and is a

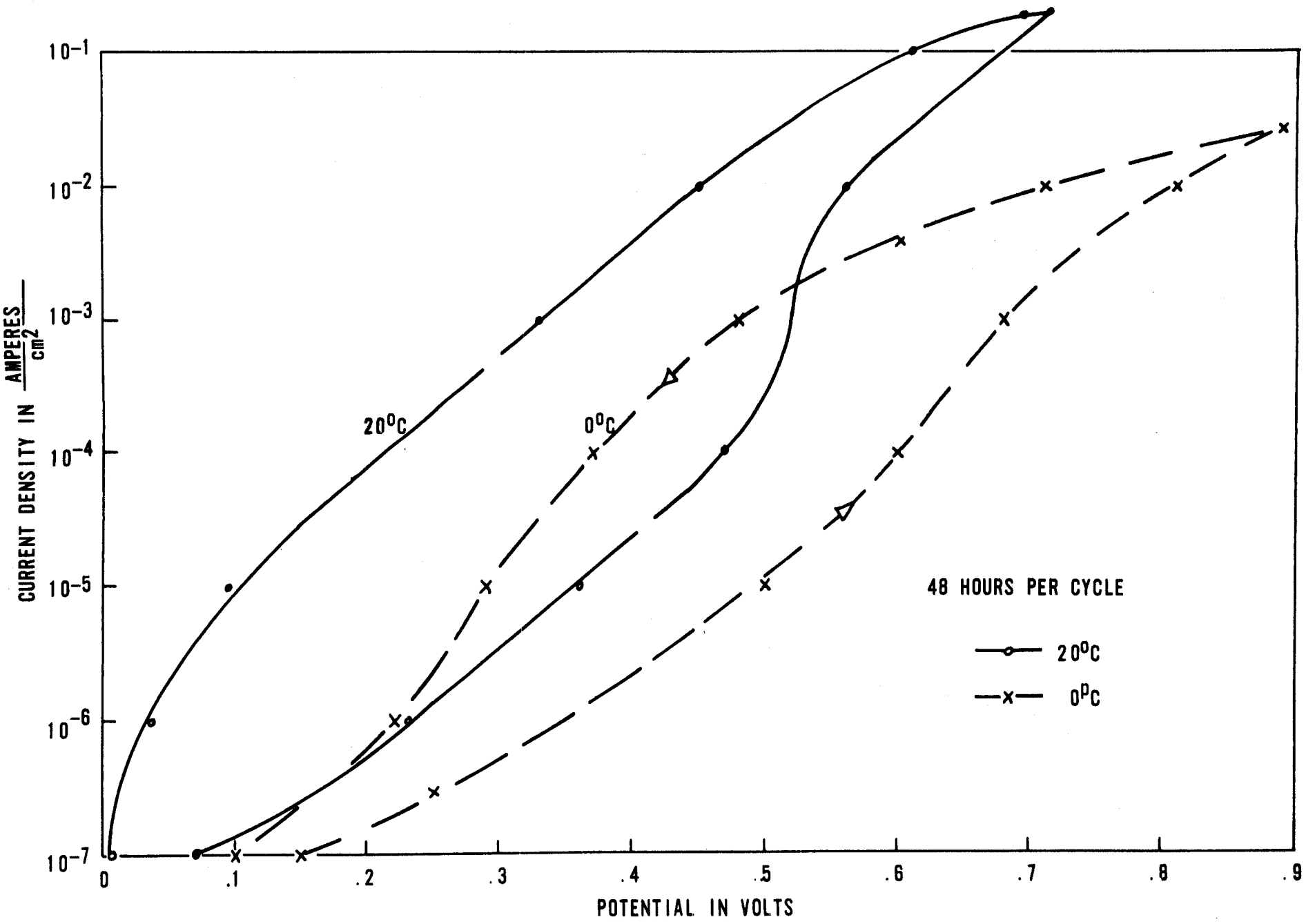

Figure 1 DARK I-V CURVES FOR CELL X39 31-2

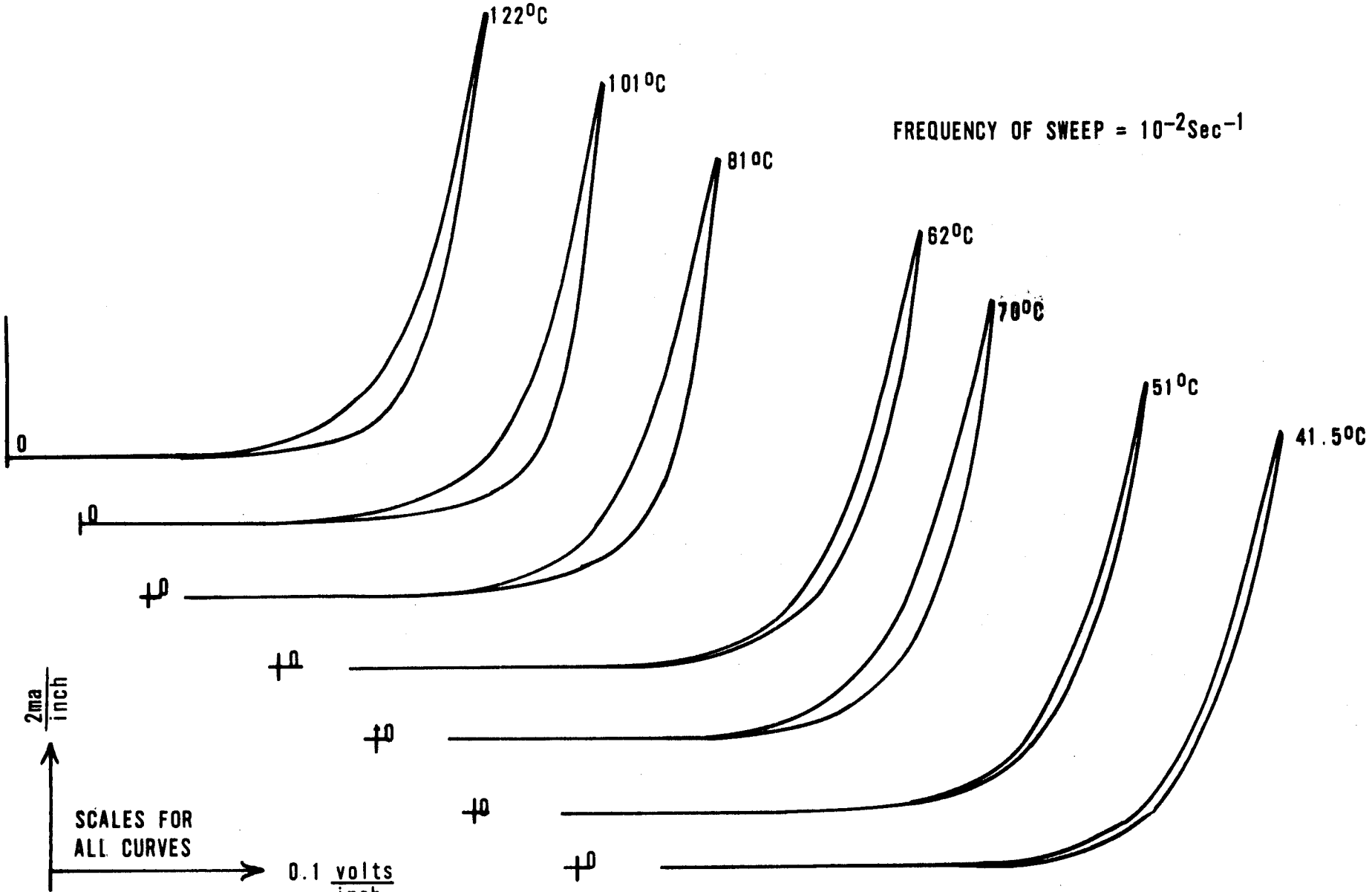

FIGURE 2 DARK I-V CURVES FOR CdS SOLAR CELL

function of the maximum voltage applied to the cell. The effect seems to be only weakly temperature dependent as is seen in Figure 2. It also seems to be greatly dependent on cell processing, as different heating cycles change the observed behavior. The hysteresis curve obtained from a given cell can be changed by varying the heat treatment. The investigation has not progressed to the point at which the curves can be used to predict cell behavior. More data is being gathered on the low frequency dependence over the range from 10^{-2} sec^{-1} to 10^{-6} sec^{-1}. Whatever the microscopic nature of the mechanism for the effect, two facts are clear: 1) If the hysteresis is in fact a steady state phenomenon, as in the case of ferromagnetism, a change of state must occur in the material of the cell. This change must be characterized by an energy which can be measured by the I-V data itself; 2) If the hysteresis is a transient effect, such as shown by RC and LC networks, a low frequency limit exists and it too should be shown in the I-V data. Hopefully, the latter case is true, since it would yield to analysis more readily than a change of state.

Measurement of these effects are underway at this time. An x-y plotter was used to record the data. A DC power supply fed from a motor driven variac served as the low frequency ramp function generator. All data were taken in the dark at room temperature. I-V curves taken under different colors of illumination will also be recorded.

Effect of CdS Surface Preparations

The first few atomic layers of the CdS thin film surface form the basis for the p-type Copper Sulfide barrier layer. The nature of the surface

therefore, plays its role in the barrier layer formation and the resulting cell. To determine cell properties as a function of the CdS thin film surface, films were lapped with 600, 1000 grids and Linde A polish. The structures of the surfaces were markedly different from each other and from that of the untreated CdS film. An indication of these differences is given by the pictures displayed below.

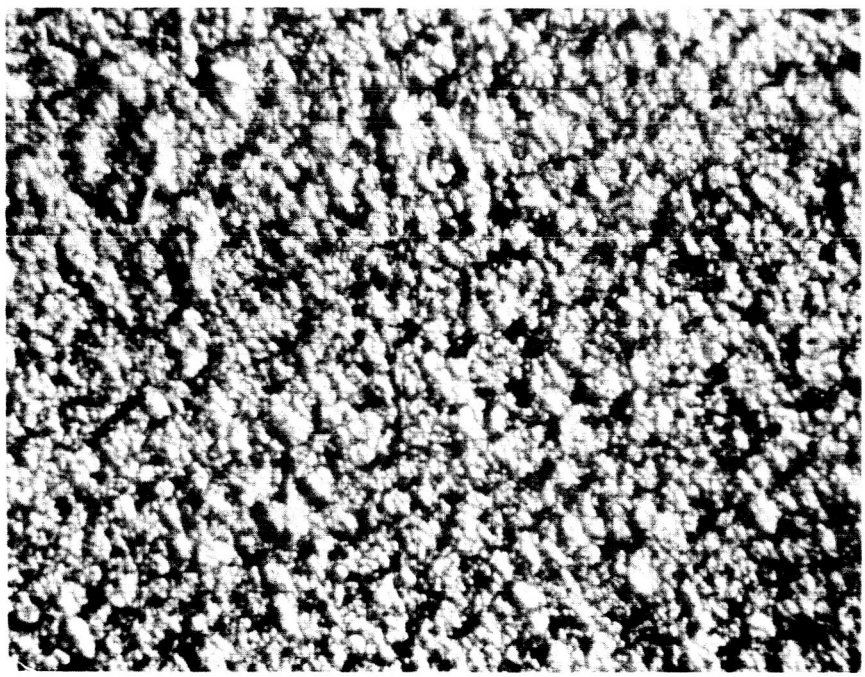

Figure 3

Untreated CdS Thin Film Surface. Magnification 320 X

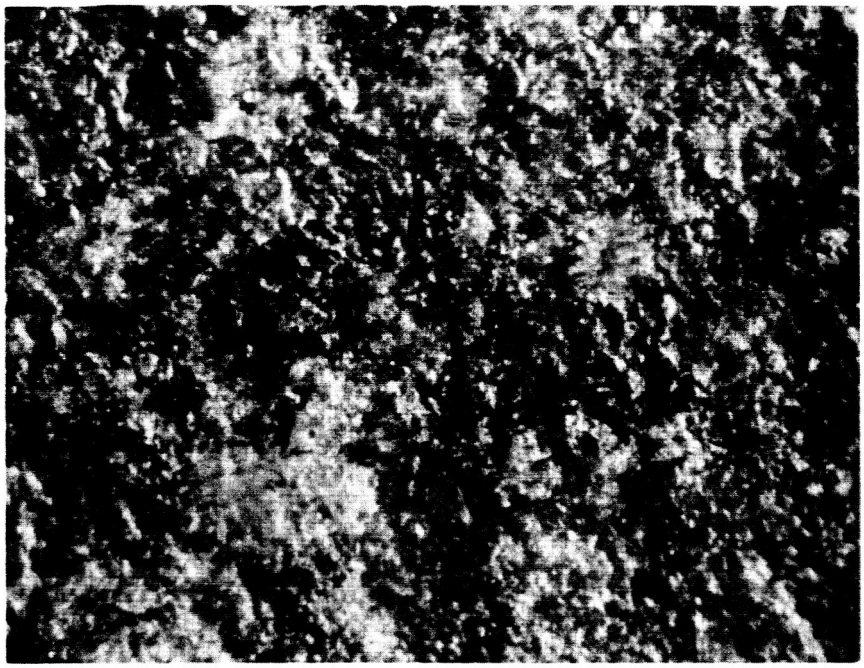

Figure 4

CdS Thin Film Surface Lapped with 600 grid.

Magnification 320 X

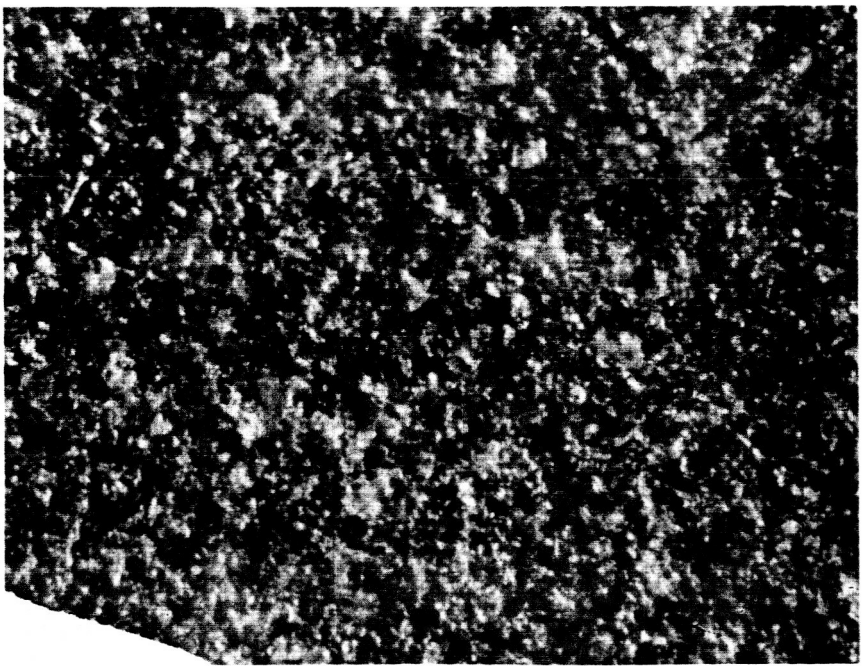

Figure 5

CdS Thin Film Surface Lapped with 1000 Grid.

Magnification 320 X

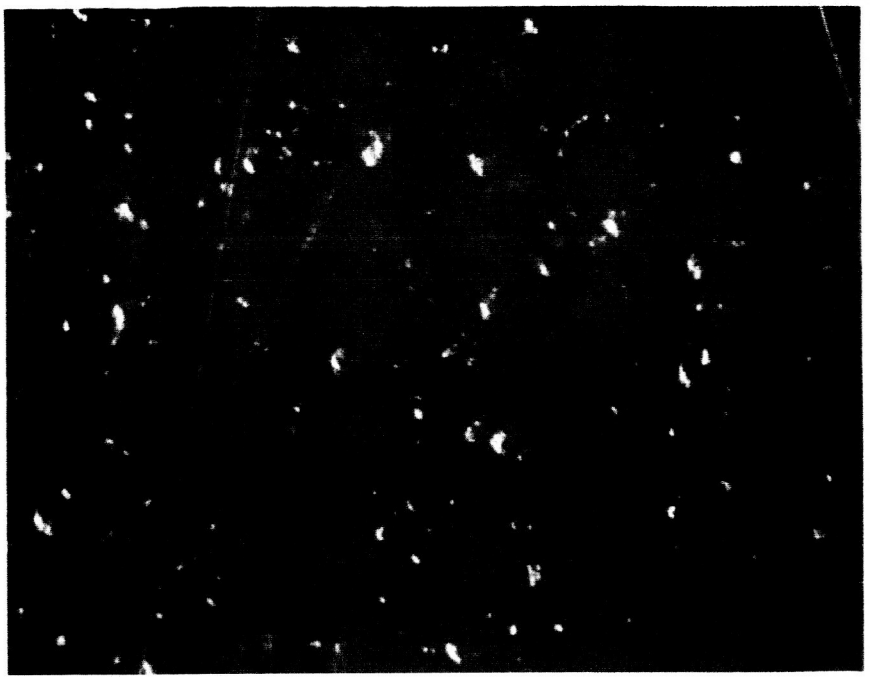

Figure 6

CdS Thin Film Surface Polished with Linde A Polish.

Magnification 320 X

Chemiplated barrier layers were formed on treated and untreated films. Measurements of the I-V characteristics illustrate a dependence of open circuit voltage and short circuit current on the nature of the CdS film surface. Additional I-V characteristic data are being compiled to define this dependence.

Etching rates of several etchants at various concentrations are being determined. Treated and untreated surfaces of CdS thin films and crystals are being etched to prescribed depths. The need for this work has been emphasized by the quality control studies being conducted on the pilot line. Unetched cells rarely equal or exceed the output of the etched cells.

Close Spaced Vapor Transport of CdS

The method presently accepted as the means of forming the CdS thin film is evaporation. The evaporation procedure involves the sublimation of the CdS at 1000°C to 1100°C from crystal chips, sintered cake or powder. Truly effective measurement and control of the various parameters is difficult. The yield of total weight of CdS as a film compared to the total weight of CdS charged into the system is on the order of 20%. As a result, the procedure causes heavy coatings of CdS over the apparatus and bell jar. Commerical production would, of necessity, require reclamation and maintenance resulting in increased costs.

The polycrystalline film resulting from this procedure has an irregular surface, see Figure 7. Uneven barrier layer formation on such surfaces result in an uneven layer thickness. Variations in cell output over the surface of the completed cell can be expected. Such variations have been observed. A method to overcome the aforementioned cell problems was desired.

Closed space vapor transport procedures have been investigated as a means of solving these problems.

During the first quarter, CdS thin films were produced on molybdenum substrates by the transport method. Much time was spent in the design and development of workable fixtures since the initial problem was to cause the transport of CdS. The next problem was to effect proper thickness and uniformity. Temperature and time of transport at 1μ pressure were investigated. Cells were made and measurements taken. Cell efficiencies are increasing as will be seen in a later paragraph.

It appears that this work may result in an improved solar cell process and product. Lower source operating temperatures, about an 80% CdS material utilization, and a soft pliable cell product are the initial benefits. Figures 7 and 8 compare an evaporated film with a transported film. Both films are c-axis oriented perpendicular to the substrate, but differ in that the transport film has 1) an obvious orientation in the plane of the photograph, 2) freedom from cracks, and 3) a low concentration of voids.

A discussion of the methods appears in the following sections.

Fixture Design

The first fixture consisted of a lower and upper strip heater at different temperatures to provide a temperature gradient necessary for vapor transport. However, the films produced were of varying thicknesses and somewhat continues across the substrate. This indicated non-uniform heat. A shallow box was made to provide increased powder exposure. See Figure 9. The box was placed on a plate directly over the heater to provide a more constant heat distribution. This was an improvement but the films still were not uniform.

After a number of modifications to the heaters, it was decided that a combination heater and powder holder was required. With this arrangment the powder was in direct contact with the heating element which developed a more constant and uniform heat while enabling a more accurate monitoring of the temperature. The films produced from this heater design are the most uniform to date.

Temperature and Time Dependence

The powder temperature was varied from 450°C to 900°C resulting in differences in the rate of transport. However, it was found that too high a rate of deposition caused the film to flake off the substrate after a thickness of approximately 25 microns was attained. Deposition times varied from 15 minutes to 90 minutes. A powder temperature of approximately 700°C, with the substrate temperature, calculated to be 654°C, was found to produce films 12 microns in thickness.

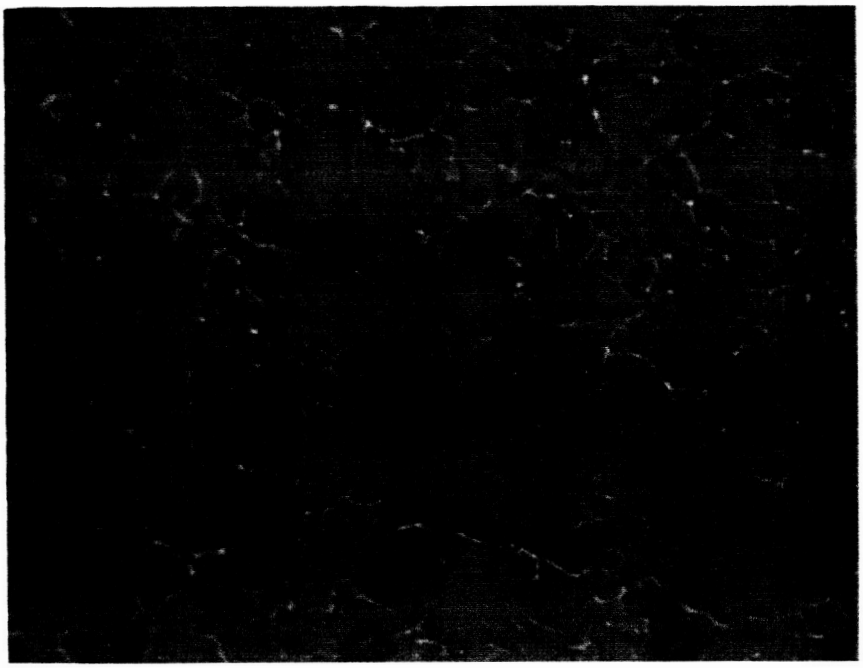

Figure 7.
CdS Polycrystalline Evaporated Film.
1000 x Magnification

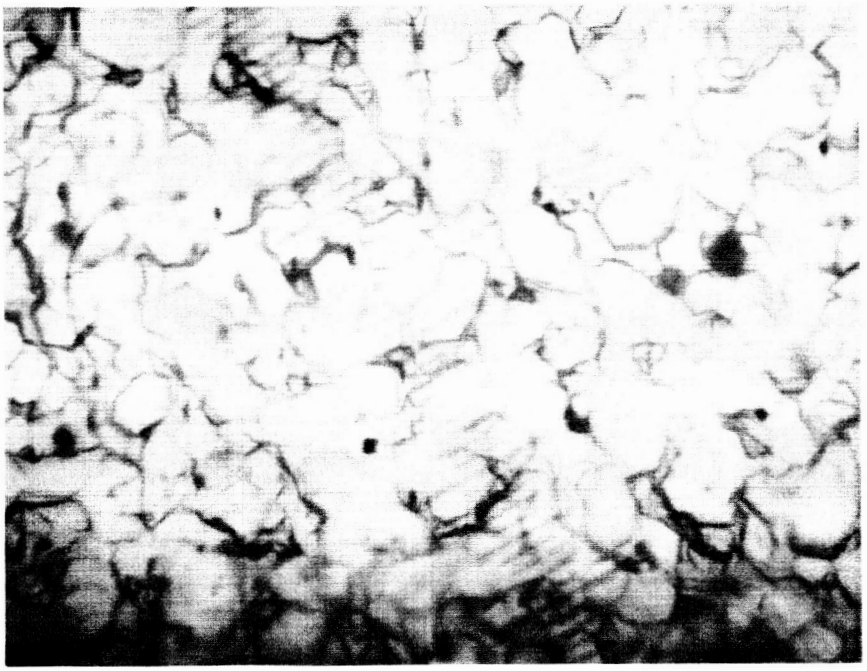

Figure 8.
CdS Vapor Transported Film.
1100 x Magnification

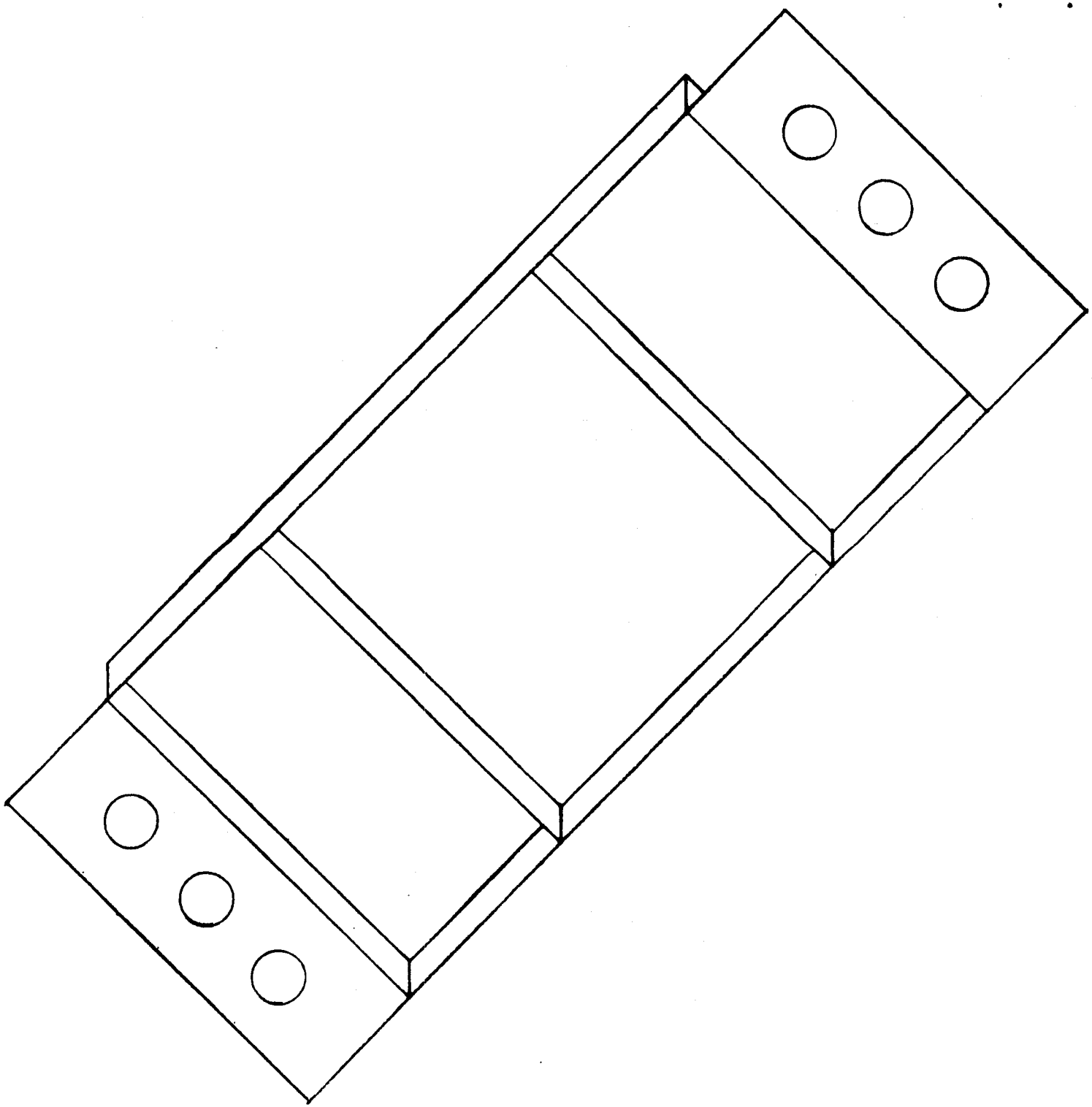

Figure 9 Vapor Transport Fixture

Cell Production

Vapor transport films produced toward the end of the quarter were considered to be suitable for cells. The results are reported in the following table. The barrier layer was formed by CuCl immersion method used for the evaporated films as reported[1].

Run #	CdS Film Thickness (microns)	CdS Film Resistivity (ohm-cm)	Cell V_{oc} (Volts)	J (ma/cm^2)	Cell Eff. (%)
22	11	1.2×10^3	.40	5.5	1.12
32	7	3.9×10^4	.40	6.9	1.90
33-C	12	1.9×10^3	.39	11.04	2.65*
33-2	12	1.9×10^3	.38	13.25	2.38*
35-1	12	0.95×10^2	.43	9.37	2.62*
35-2	12	0.95×10^2	.40	11.8	2.89*
35-3	12	0.95×10^2	.40	13.6	3.52*

*Efficiencies measured after lamination

The adherence of the above films was exceptionally good as evidenced by the fact that a 10μ film cell on a 0.002 in. Mo 3" x 3" substrate was bent nearly 180° before evidence of cracking appeared. Cracking appeared after folding and pressure was being applied to cause a crease in the substrate.

The crystal orientation is much like that of the evaporated films with the c-axis of the crystallites perpendicular to the substrate.

During the next quarter, additional work will be done on the powder holder and heater. Cells will be made and investigated to determine a maximum efficiency and spectral response.

Vapor Transport of Cu_2S

A cross section examination of a thin film CdS solar cell reveals the dark irregularly shaped barrier layer that has been formed in the top surface of the CdS. No photograph is presented because black and white prints do not make this apparent. Nevertheless, large variations in the barrier thickness cause appreciable variations in the cell output per given area.

Formation of a precise uniform thickness of cuprous sulfide as a barrier layer should provide a cell of uniform output. Formation of a Cu_2S layer ought to be accomplished by a means of vapor transport since it deposits layers very much like the charge materials whereas evaporation does not.

The method [2] proposed for this work was described by Nicoll. The powdered material to be grown is placed in the bottom of a flat, shallow box. The cover of the box serves as the condenser (substrate). Large flat heaters maintain the cover and the box as isothermal surfaces. The substrate is maintained about 50°C cooler than the powder layer. The powder evaporates from the shallow box and condenses on the substrate. This closely approaches equilibrium conditions and large crystallites result. Conductivity is controlled by the addition of dopants to the powder.

It is conceivable that a barrier can be deposited on the CdS thin film to form a front wall type cell, or can be applied to a substrate initially, followed by a CdS layer, to form a rear wall cell. It is intended to study both types.

The advantage of the rear wall configuration is that the lower conductivity Cu_2S is in contact with a sheet of metal (substrate) and the higher conductivity CdS is on top. This allows the use of larger collector grid openings with a resultant increase in exposed active area.

It was felt that in order to apply the above system, it was necessary to obtain data on the dependence of transport velocity on the iodine pressure and the substrate and powder temperatures. Such data is more easily obtained in a somewhat different system.

First, a flow system was examined. A pyrex tube closed at one end and pumped at the other was placed in a tube furnace so that the center of the tube containing a polycrystalline disc of cuprous sulfide was maintained at 350°C. At the closed end of the tube, iodine crystals evaporating from a graphite cup at room temperature furnished a stream of iodine vapor which passed over the cuprous sulfide to a cold trap. Some etching of the cuprous sulfide was observed. However, study of the literature(3) on vapor transport of semiconducting compounds suggested that a closed system would be more suitable for these studies.

Therefore, two small two-zone furnaces were assembled by winding nichrome ribbon around a quartz tube which was then slid inside a larger quartz tube to reduce radiation heat loss. Associated power supplied and controllers independently controlled the temperature of each zone. Temperatures could be maintained as high as 1050°C.

Varying amounts of Cu_2S (prepared by passing H_2S over semiconductor grade Cu at 800°C) and I_2 were sealed into small (5mm x 6") quartz tubes. The tubes were placed in the two-zone furnace. With the Cu_2S at 580°C and the cold end of the tube at 450°C, considerable numbers of blade platelets formed at the cold end of the tube and small crystals formed on the Cu_2S source material. In subsequent experiments at higher temperatures, larger crystals were grown at the cold end of the tube, one of which is shown in Figure 9.

The data obtained so far, although qualitative in character, suggests that high temperatures on the order of 900-1000°C and low iodine pressures on the order of 20mm of Hg are necessary to obtain an appreciable transport velocity.

Electrochemical Etching of Substrates

The weight of the CdS cell has been reduced by controlled electrochemical or chemical etching of the molybdenum substrate. The molybdenum substrate can be reduced to less than 1 mil thick without harm to the CdS cell. This weight reduction in turn yields a higher watts per pound value for the solar cell.

Initially, the cells were chemically etched using a 50% nitric acid solution followed by a rinse in hydrochloric acid. This method of etching has had limited success due to uneven etch rate. As a result of this uneven etch rate, it was difficult to etch the molybdenum substrate below 1.0 mil in thickness.

In order to obtain control of the etch rate and safely reduce substrate thickness to $\frac{1}{2}$ mil, electrochemical etching of molybdenum sheet was selected. The exposed surface of the molybdenum served as the anode. A carbon electrode served as the cathode. The amount of metal electrochemically etched away

1 mm

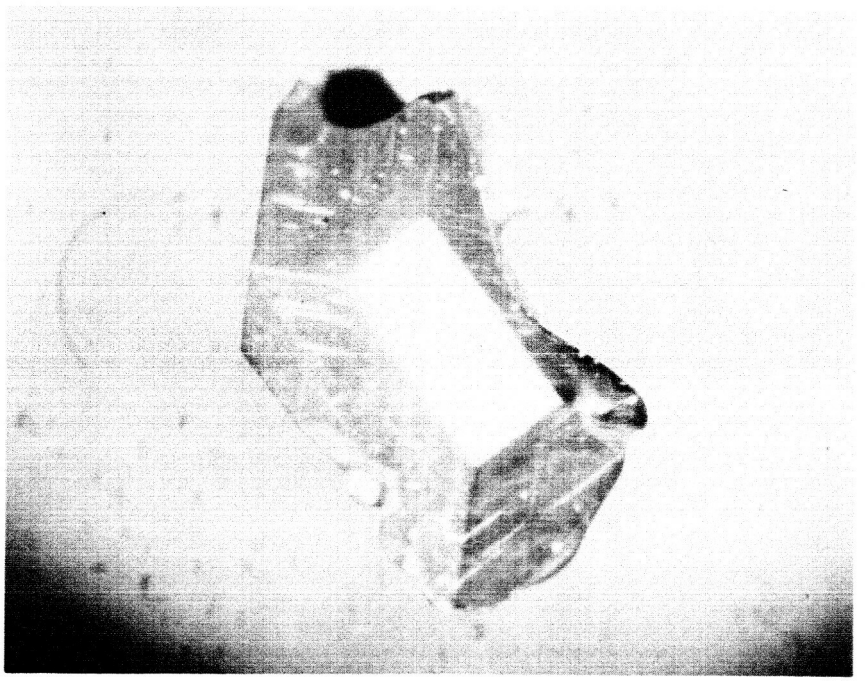

Figure 10

Vapor Transported Cu_2S Crystal

obeys Faraday's Law.

In preparation for etching of the molybdenum, the samples were degreased in Acetone, Trichloroethylene and Methanol. The samples were cleaned successively by HNO_3, water, chromic acid, and NH_4OH, with a final rinse in alcohol. A 20% Potassium Hydroxide was selected as the electro-chemical etch solution.

A Hull cell (267 ml capacity) was used for the initial work of electro-etching the molybdenum. With a Hull cell, a record was obtained of the etch rate on the sample at all current densities within the operating range. Results so far indicate that the electro-chemical etching produces an etched surface without excessive surface roughness or pitting. It was determined that a current density of 200 ma/cm^2 yields an etch rate of 0.1 mil per min.

The main problem encountered with the electro-etch experiments seems the "edge-effect" or accelerated etching at the corners and edges of the molybdenum sample. This results in a perforation of the Mo along the edges and an attack on the CdS cell. Reduction of the cathode size and changing the distances between the anode and cathode has reduced the problem. Further reshaping is still required.

Collector Grids

Gold Electroformed

As a quality control check of incoming material, the physical dimensions and weight of the Buckbee-Mears 70 line per inch gold grid was determined. From these figures, a density of 7.5 gms/cm^3 was obtained for the grid lines. This is less than one half of the handbook value of 19.3 gms/cm^3. Also, the sheet resistivity of this grid is ten times greater than the calculated

value of 10^{-2} ohms per square. (Calculation based on resistivity of bulk gold.) Both the low density and the high resistivity illustrate the porous nature of the electroformed grid. Attempts to prepare a sample of our electrodeposited grid for sheet resistivity measurement for comparison with the commercial grid, have failed thus far due to difficulties in removing the grid from the substrate. Some success has been obtained by etching away a thin copper substrate on which the grid has been electrodeposited. However, subsequent handling of the grid is very difficult. This problem should be solved by using an etching technique which leaves a peripheral metal support. Once a procedure for sheet resistivity has been established, various electroplating techniques can be evaluated using the sheet resistivity as a standard.

Electrodeposited Grids

Various improvements in the grid electroplating process have led to higher yields as well as more favorable electrical and physical characteristics. The improvements are due to thicker photoresist masks, vigorous air agitation of the gold alloy plating bath, and low initial plating currents which are described below. The yield attained thus far is 67%.

Photoresist Masking

Because of the difficulties in masking the pinholes and in grid line definition, a thicker photoresist coating was applied. This was accomplished by using a multiple coat method with decreasing spinner speed. Resulting masks have fewer pinholes requiring touch-up with a brush and photoresist. The effectiveness of this improvement can be judged by an almost complete elimination of "shorted" cells after grid electroplating. The thicker photoresist mask also gives a better defined grid because the lines remain of uniform width as the thickness of the line increases.

Additional air filtration has been installed in the darkroom in an effort to reduce dust contamination. Dust particles cause holes in the resist mask.

Electroplating Solutions

Modifications in the plating procedure have also contributed to the increased yield. The increase may be due to an improved contact between the cell and the gold grid. The procedure now requires an initial deposition of a thin 24K gold layer followed by a thicker high conductivity gold alloy layer. Now, the initial plating current in both baths is 10% of the final plating current. This gradual increase in current allows the first layer of the plate to conform closely to the texture of the surface to be plated thus insuring a better contact. Air agitation of the gold alloy bath has eliminated fogging.

A new high speed gold plating solution Sel-Rex, Temperex HD, was tested by plating a cell. Although this cell was merely a mechanical sample with low power output, no power decrease was observed. More important, photomicrographs showed that a deposit approximately twice as thick as normal was obtained in the same plating time. Normal deposits are 2.2 microns thick.

Investigation of this plating solution will continue.

Yields

A bar graph, Figure 10, illustrates cell performance before and after plating. The "acceptance" line is drawn at minus 5% because this is a reasonable margin of error in cell testing. Earlier estimates of yield were based on cell survival. The yield is expected to rise because twelve out of the last fifteen cells processed (80%) were acceptable.

Further Work

Investigation of plating techniques and solution will continue.

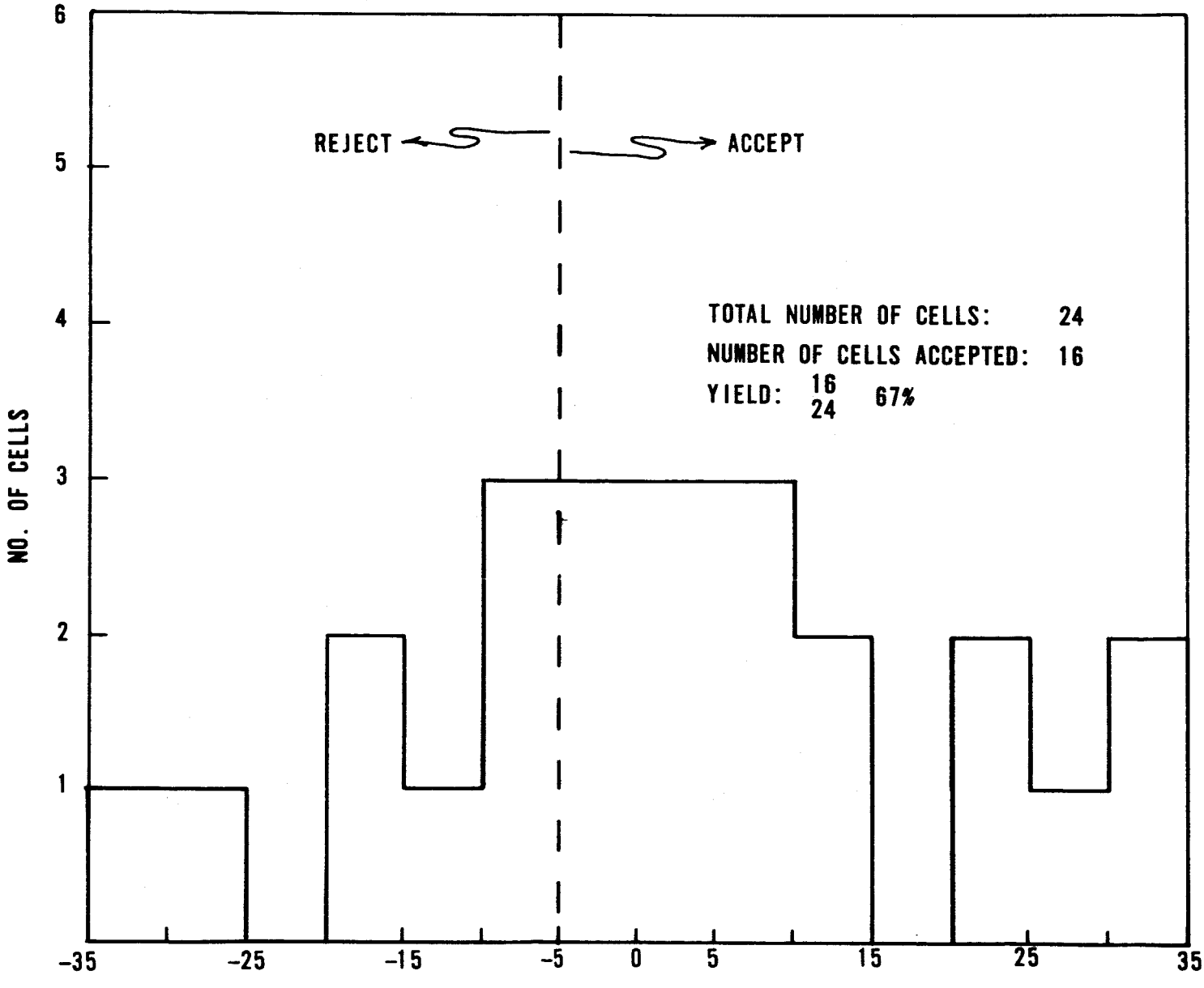

FIGURE 11 PERCENT CHANGE IN CELL EFF. DUE TO PLATING

Contoured busbars, tailored in dimensions to the total current carried, will be investigated. Sheet resistivity samples will be prepared.

Semitransparent Films

Semitransparent films are being applied to the surface of the CdS solar cell with the purpose of providing increased collection efficiency. The layers to be investigated are CdTe, CuTe, Bi_2O_3 and Au.

Several evaporations of CdTe were made on glass to determine the best thickness and conductivity. The following table shows several of the CdTe films on glass. All of the films are n-type.

No.	Substrate Temp.	Filament Temp.	Doping	Thickness	Avg. Trans-Mission in Visible	Resistivity (ohm-cm)
23	300°C	950°C	.1% CuCl	800Å	56%	2.35×10^4
49	100°C	950°C	.1% CuCl/ 30% Te	400Å	28%	Not Measured
50	100°C	950°C	"	200Å	30%	" "
51	100°C	950°C	"	100Å	92%	1.3×10^3

Films of CdTe were applied to eight CdS film cells according to the conditions reported for film No. 51 in the table. A large transmission variation of about 30% was apparent probably due to the difficulty in controlling the great excess of Te in the films. All of the coated cells suffered loss of both current and voltage. Their I-V curves displayed increased series resistance. No further work on the CdTe film as a semi-transparent collector is anticipated.

Further work in this area will follow in order, CuTe, Bi_2O_3 and Au.

Interface Materials

In order to provide an ohmic and tightly adhering contact between the CdS and the substrate, several interface materials are being investigated. Sputtering techniques are being used to provide metallic coatings on molybdenum. Greater adhesion of the coatings is anticipated. Electrodeposition of materials on molybdenum is difficult and generally lacks adhesion. The following results have been obtained:

Gold - Layers of gold less than 0.5 mils were sputtered on 2 mil molybdenum. Three such 3" x 3" substrates were put into a vacuum chamber. Glow discharge was used to clean the surface before the CdS was evaporated. The CdS adhered well to the gold coated molybdenum. However, there was no indication of an improved ohmic contact since the control cell displayed a better I-V characteristic. Gold will also be sputtered on substrate materials other than molybdenum.

Silver - Layers of silver less than 0.5 mil were sputtered on 2 mil molybdenum. Seven substrates were prepared and coated with CdS after a glow discharge cleaning. Two cells 4.8% and 4.6% resulted. In all cases, those with sputtered silver were better than the control. More cells will be made using sputtered silver as an interface.

Zinc - Several attempts were made to sputter zinc on the molybdenum. The zinc would not deposit on the molybdenum.

Copper - Layers of copper less than 0.5 mil were sputtered onto 2 mil molybdenum. It adhered well. However, when the CdS was evaporated, it reacted with the copper to form a grainy brown film. This film was easily separated from the molybdenum, showing a gray layer next to the molybdenum.

Sputtered copper was also used as a base for layers of electroplated cadmium, zinc, silver and additional copper. In each case, however, the copper tended to blister and peel from the molybdenum. For this reason, cells could not be made. It did suggest that copper foil be plated with various metals and used as a substrate in place of the molybdenum. This is now being done.

In conclusion, the only interface material that shows promise is silver. The investigation will continue.

Quality Control in Cell Fabrication

A portion of the work on this program requires a quality control study for cell fabrication. Such studies are helpful in determining criteria for acceptable production with respect to quality and cost. The results are as follows.

The acceptable bulk properties of the CdS thin films produced by evaporation are generally less than 1000 ohm-cm. Large changes in resistivity have little effect on the final cell quality. It appears that the last few atomic layers of the film surface controls the cell quality. This layer is of great importance since it is used to form the p-type copper sulfide barrier layer.

Source temperature or boat temperature control has always been a problem. Presently voltage and current readings are being taken at the boat terminals and the total power is being calculated. The calculated temperatures are being compared to readings obtained with an optical pyrometer.

Etching of the CdS surface invariably assists the formation of the barrier layer resulting in higher quality cells. Work is being conducted

on lapping and etching of the surface and is reported elsewhere in this report.

The bath temperature during the barrier formation was dropped to 65°C from 85°C to enable the operators to exercise more control. An unexpected result was a temporary drop in the average efficiency to 3%. Previous data had shown a nearly straight line time-temperature relationship for immersion. The temperature has been re-established at 85°C. The pilot line serves as a source of films and cells for the entire project. Each evaporation has a process record sheet showing all pertinent data and its eventual usage or completion as a cell.

A large nitrogen-filled dry box has been built and put into service for assembly of cells and arrays. Degradation during assembly should be greatly reduced. All materials used in such assemblies are stored in the box prior to usage.

Thirty-seven 6" x 6" films, equivalent to 148 3" x 3" films have been evaporated on the pilot line.

123 films were supplied for research and development purposes.

Twenty-five cells were made from films.

5.6% was the maximum efficiency.

4.3% was the average efficiency.

2.7% was the minimum efficiency.

REFERENCES

		Page
1	J. C. Schaefer & R. Statler, "Recent CdS Solar Cell Developments," Vol. II, A-7. Fourth Photovoltaic Specialist Conference, June 1964, NASA-Lewis Research Center, Cleveland, Ohio.	15
2	Nicoll, F. H. J. Electrochem. Soc. 110 (11), 1165 (1963)	16
3	I.B.M. J. Research and Development, Vol. IV, No. 3, July 1960. Special issue devoted to vapor transport.	17

A MODEL FOR THE CdS SOLAR CELL*

E.R. Hill & B.G. Keramidas
Harshaw Chemical Co.
Cleveland, Ohio

October 1965

*Research supported by grant from The Harshaw Chemical Company and contracts from NASA, Lewis Research Laboratory and Wright-Patterson AFB.

The CdS solar cell in its present form consists of a film or sheet of CdS which has had one face chemically treated to form a rectifying junction. The treatment consists of an immersion of the CdS in an acidified hot water solution of Cu_2Cl_2. The chemical reaction is described by the upper equation in Fig. 1. Thermodynamically, the reaction proceeds to the right, since that side of the reaction has a lower free energy. Kinetically, the reaction is aided by $CdCl_2$ dissolving in the water solution. The equilibrium concentrations of the four reaction components are governed by the lower equation (the Nernst relation), where the right hand member is a function of temperature only. For discussion purposes, the Cu^+ ion and the Cd^{2+} ion can replace the Cu_2Cl_2 and $CdCl_2$ in both equations and retain approximately the same thermodynamic properties.

Cu_2S as made in above manner is a p-type semiconductor with a band gap near 1 eV and a hole concentration of about 10^{20} per cm . The CdS is n-type with a band gap of 2.4 eV, and generally has an electron concentration of about 10^{18} per cm^3. Consequently, if these two materials can be joined with the proper physical arrangment, a rectifying junction should result. This does take place since an evaporated CdS film which is treated chemically and electrically contacted has the electrical character of a diode. This diode is usually rather leaky and has a high saturation current on the order of microamperes per cm^2. When illuminated, it generates current, the spectral response of which is shown in Fig. 2. Nothin unusual is present in this response except at about 1 eV, and it is concluded that the active material has a 1 eV optical bandgap. We can also conclude that CdS is not optically active since no change in response occurs at 2.4 eV. This has described the overall nature of the materials, processing and end product.

To understand the more detailed nature of the cell, it is necessary to examine the process on a microscopic level. The chemical reaction is a double displacement type which requires that each time two Cu^+ ions enter the CdS film, one Cd^{2+} ion must leave. If the CdS is highly ordered as in the case of a single crystalline face, only a few monolayers of Cu_2S are formed. This is to be expected since few sites of high chemical activity such as dislocations and grain boundaries are present. Also, the reaction takes place at a temperature around 100°C, and the diffusion coefficients of the components in CdS will be low. However, if the CdS is highly disordered, as in the case of a polycrystalline film or a lapped single crystal, regions of high chemical activity are plentiful and diffusion is enhanced by the presence of grain boundaries and dislocations. In fact, chemical action is seen to penetrate to depths of several microns in evaporated films.

In order for the chemical reaction to occur past the solid surface, diffusion of the reactants must take place, which implies concentration gradients. Fig. 3 shows a schematic picture of the CdS cell cross section representing the cell at any time after immersion in the solution. As can be seen, a gradient of Cu^+ ions and Cu_2S extends into the CdS and a gradient of CdS and Cd^{2+} ions extends out to the surface. These gradients must exist for the reaction to proceed at all, and consequently must exist in the cell when it is removed from the solution. When it reaches thermal equilibrium after the chemical treatment, it will still be in a state of chemical non-equilibrium, since the concentration gradients are still present. This can be called a state of quasi-chemical equilibrium, i.e. over a small region, the Nernst relation governing the component concentrations will be only slightly perturbed. Ultimately, in deference to the second law of thermodynamics, a state of equilibrium will be reached where all four reaction components are uniformly distributed throughout the solid and are in equilibrium with their vapor state. The rate at which this condition is approached is determined by the mobilities and concentration gradients of the species and the temperature. At room temperature, this occurs very slowly, but over a period of weeks, it can be detected.

When the cell is heated, however, this tendency is accelerated and five minutes at 300°C produces a marked change. It is unlikely that the Cu_2S and CdS molecules will be particularly mobile, but Cd^{2+} and Cu^{+} ions can move. They will slide down their gradients, increasing the Cu^{+} concentration inside and increasing the Cd^{2+} concentration near the surface. The Nernst relation says there will also be an increasing CdS concentration near the surface and increasing Cu_2S concentration deeper in the cell. Fig. 4 shows the spectral response of the cell in this condition. The most significant feature is the step at 2.4 eV which says that carriers are produced in CdS within a diffusion length of the electrical junction. The I-V curve shown in Fig. 5 indicates a reasonably good diode and a true generated short circuit current. From this, we conclude that all the light which is being absorbed is absorbed within a diffusion length of the junction.

If this cell is further heated for 1 hour at 300°C, the gradients of concentration will become even flatter. The electrical junction should correspond to the region of chemical transition and will then become broader. Itwill also move further into the bulk CdS. Fig. 6 shows the spectral response of a cell subjected to such a treatment. Again, the most striking feature is the behavior at 2.4 eV where there is now almost a complete loss of response. Evidently a great deal of CdS has formed near the surface and the junction is deep inside the cell. The I-V curve, shown in Fig. 7, indicates a relatively low collected short circuit current and even begins to look like two junctions may be present. Thus, photons with energy above 2.4 eV are absorbed near the surface with a low resulting quantum yield. This low yield can be due simply to having the junction far inside the cell or to the presence of a second junction in the opposite direction.

Further heating causes additional change and after 15 minutes at 600°C the cell is useless as a power converter, but has developed a very interesting behavior. Fig. 8 shows the spectral response of the generated current which can be seen to reverse direction with color of illumination. For red and infra-red light, the current is of the sign produced by the cell initially. That is, the treated surface is positive and the bulk CdS negative. For green and blue light, the polarity reverses. For tungsten illumination, the net current is generally reversed from that of the normal cell. Red light is weakly absorbed and generates carriers deep in the cell near the normal Cu_2S-CdS junction. These carriers are separated and produce normally directed current. Green light is more strongly absorbed near the surface and produces oppositely directed current. This can be due to either non-uniform absorption as in the Dember effect, or due to the presence of a second junction with the opposite sense. Further heating merely results in material homogenization and loss due to evaporation.

This has been a sketchy discussion of the CdS cell fabrication in that only a few salient points have been examined and many microscopic details have been glossed over. For instance, Cu_2S and CdS are only weakly soluble in each other and undoubtedly the chemical transition region is composed of aggregates of clusters. On the atomic scale, this is a discontinuous structure, but on the scale of the Debye length for carriers, this is small. Likewise, the transport equation for the heterojunction has been neglected, and the assumption made that a junction exists in a chemical transition region.

The important point is that the device is the result of a double displacement chemical reaction which stops before equilibrium is reached. Thus, concentration gradients of the reactants exist in the region of chemical change. Since the initial reaction occurs near room temperature, even moderate heating can be expected to alter the distribution of the reactants. From the Nernst relation and

a knowledge of the gradients, the direction of material redistribution can be predicted. The behavior of the cell after various heating cycles can be correlated with the qualitative picture of the material distribution and their electrical and optical properties.

Finally, it is reasonable to expect this type of analysis to be suitable for application to many of the semiconductor devices where a low temperature chemical reaction takes place.

$$Cu_2Cl_2 + CdS = Cu_2S + CdCl_2$$

$$\Delta F^\circ \ (298^\circ K) = -12 \ \frac{kcal}{mole}$$

$$\ln \frac{[Cu_2Cl_2]\ [CdS]}{[CdCl_2]\ [Cu_2S]} = + \frac{\Delta F^\circ}{RT}$$

Figure 1

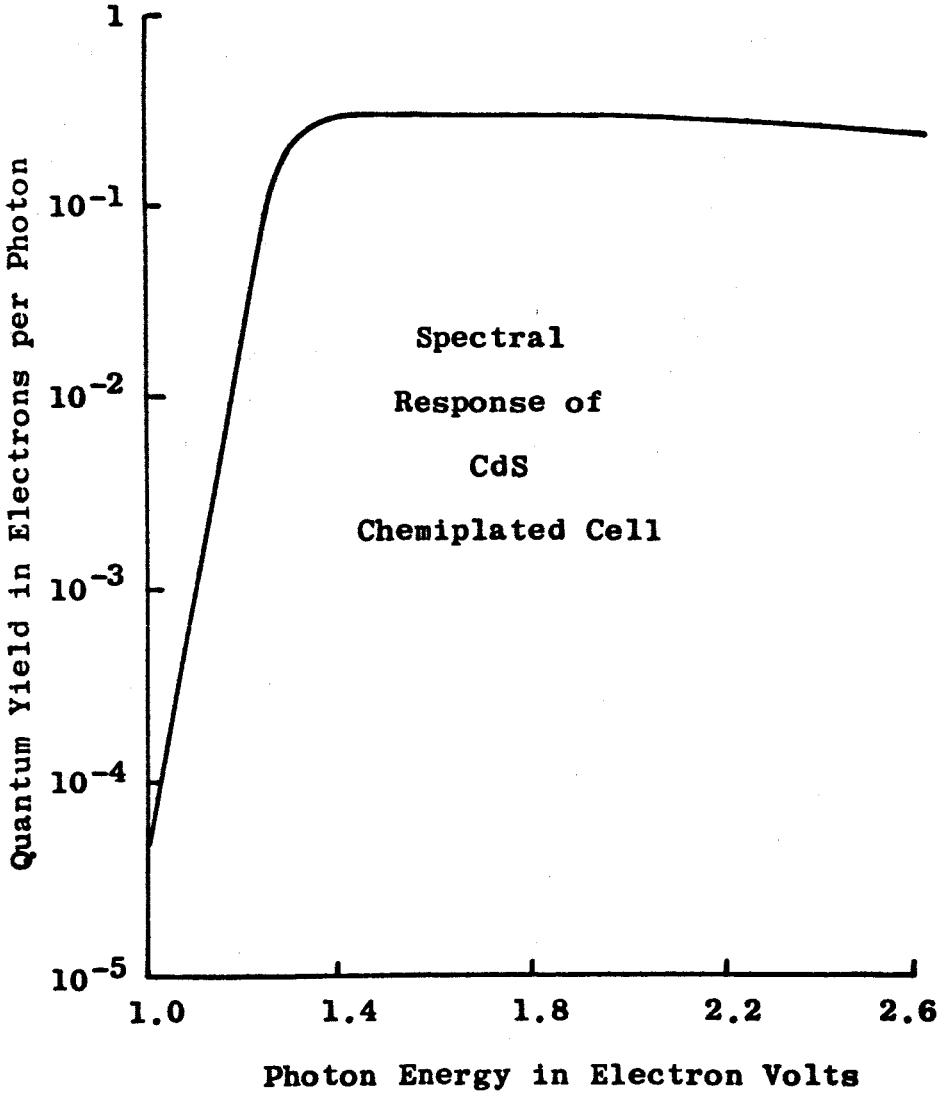
1
10^{-1}
10^{-2}
10^{-3}
10^{-4}
10^{-5}
Quantum Yield in Electrons per Photon
Spectral
Response of
CdS
Chemiplated Cell
1.0
1.4
1.8
2.2
2.6
Photon Energy in Electron Volts

Figure 2

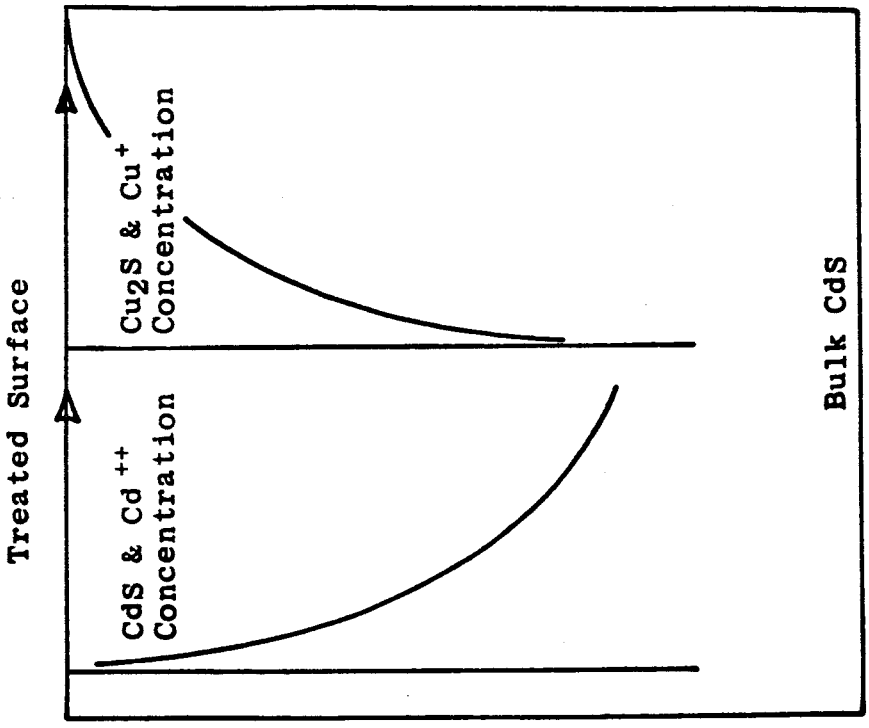

Schematic Cross Section

of Cell Junction

Figure 3

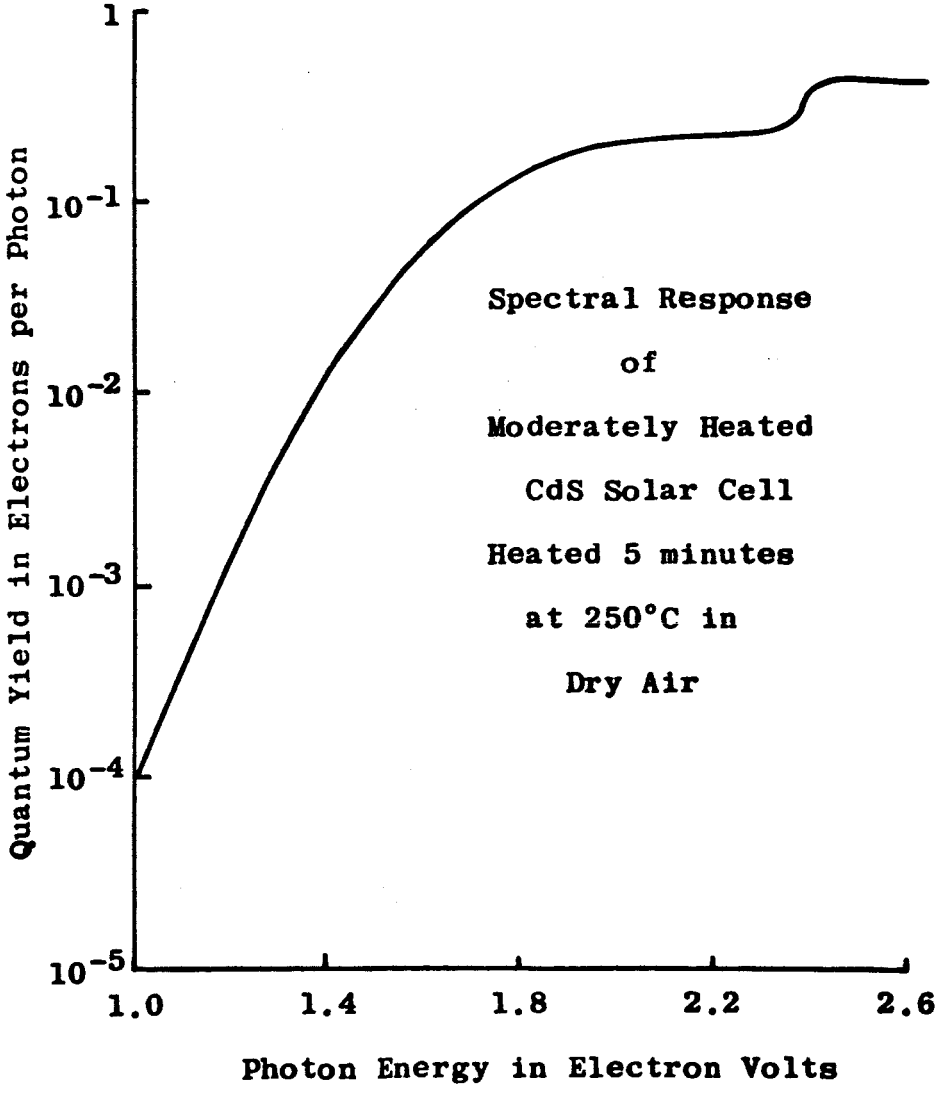
1
10^{-1}
10^{-2}
10^{-3}
10^{-4}
10^{-5}
Quantum Yield in Electrons per Photon
Spectral Response
of
Moderately Heated
CdS Solar Cell
Heated 5 minutes
at 250°C in
Dry Air
1.0
1.4
1.8
2.2
2.6
Photon Energy in Electron Volts

Figure 4

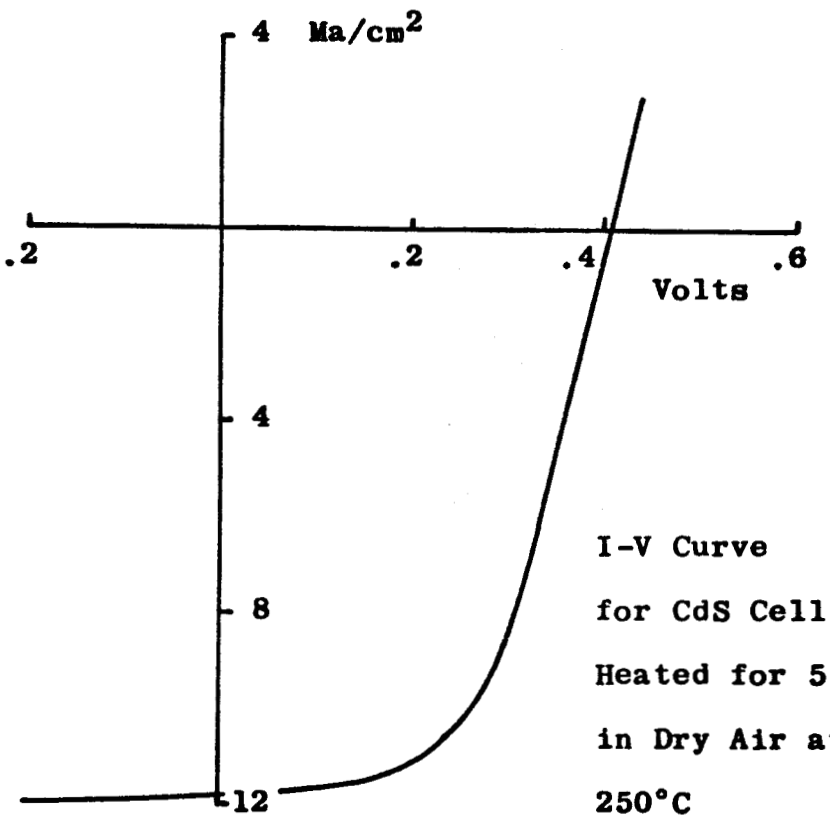
4 Ma/cm2
.2
.2
.4
.6
Volts
4
8
12
I-V Curve
for CdS Cell
Heated for 5 min.
in Dry Air at
250°C

Figure 5

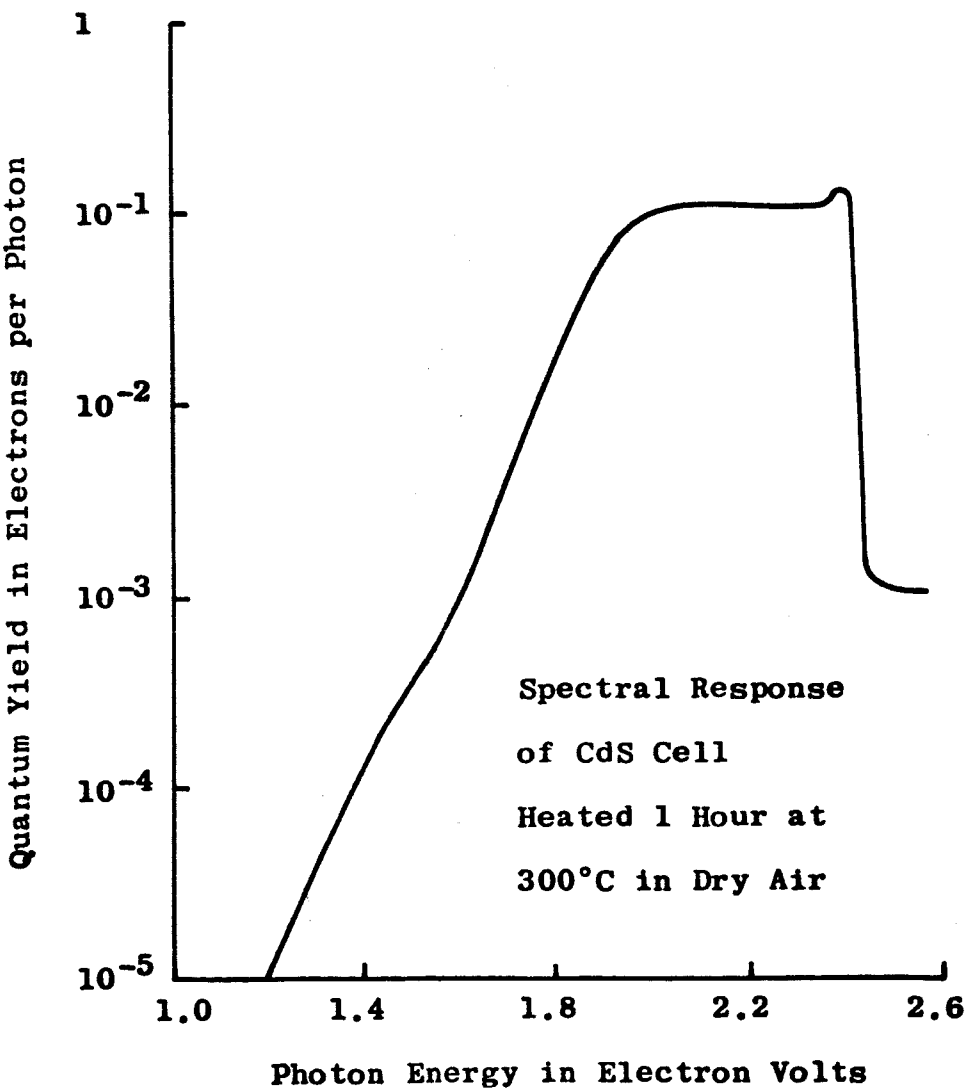
1
10^{-1}
10^{-2}
10^{-3}
10^{-4}
10^{-5}
Quantum Yield in Electrons per Photon
Spectral Response
of CdS Cell
Heated 1 Hour at
300°C in Dry Air
1.0
1.4
1.8
2.2
2.6
Photon Energy in Electron Volts

Figure 6

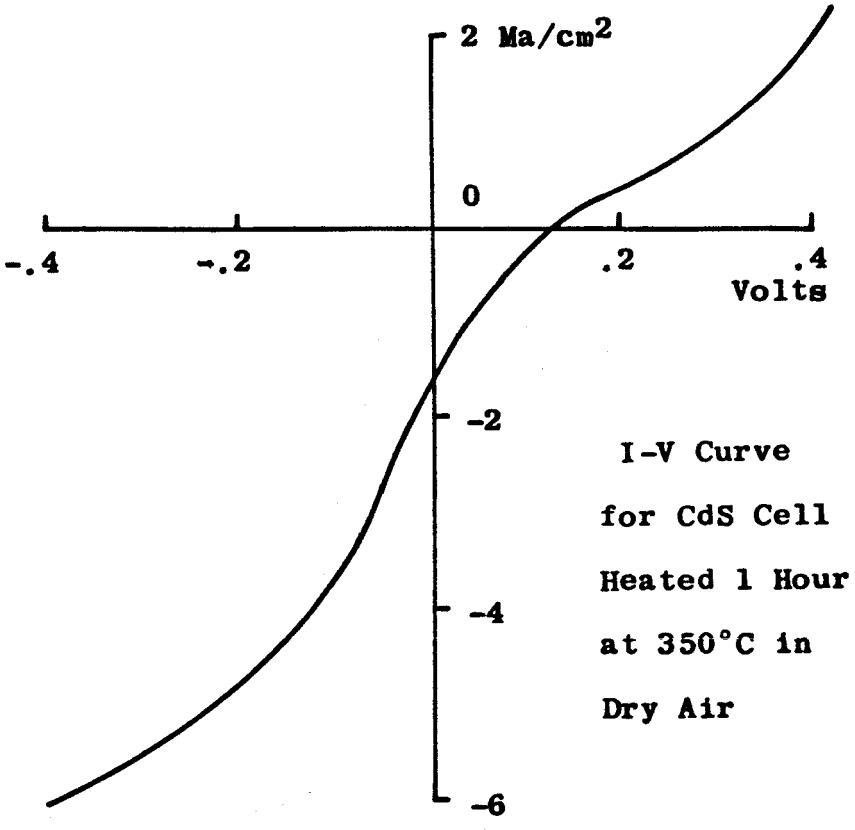
2 Ma/cm2
0
-.4
-.2
.2
.4
Volts
-2
-4
-6
I-V Curve
for CdS Cell
Heated 1 Hour
at 350°C in
Dry Air

Figure 7

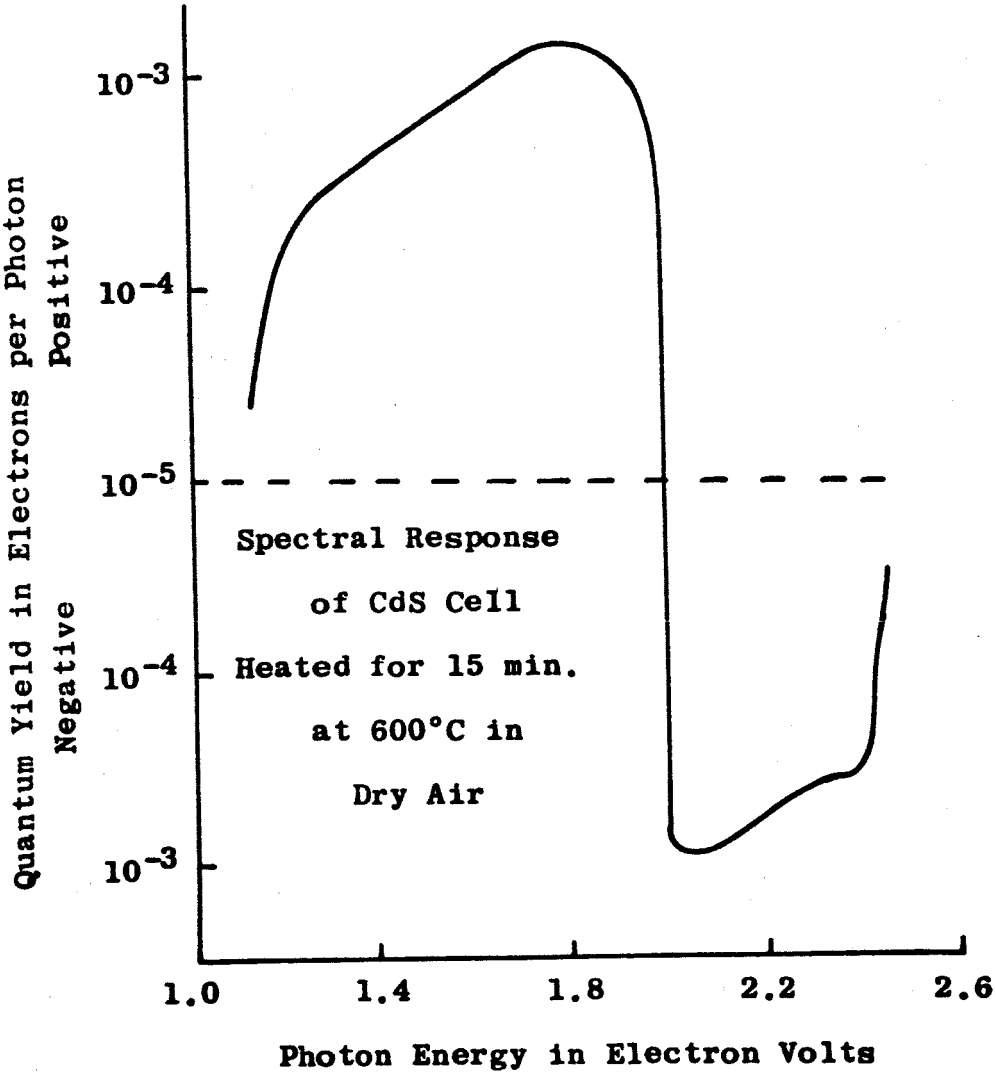
Quantum Yield in Electrons per Photon
Positive
Negative
10^{-3}
10^{-4}
10^{-5}
10^{-4}
10^{-3}
Spectral Response
of CdS Cell
Heated for 15 min.
at 600°C in
Dry Air
1.0
1.4
1.8
2.2
2.6
Photon Energy in Electron Volts

Figure 8

THE HARSHAW CHEMICAL COMPANY
CONTRACT NAS3-7631
DISTRIBUTION LIST

QUARTERLY AND FINAL REPORTS

National Aeronautics and Space Administration
Washington, D.C. 20546
Attention: Arvin H. Smith/RNW (2)
H. B. Finger/RP
Millie Ruda/AFSS-LD

National Aeronautics and Space Administration
Scientific and Technical Information Facility
P.O. Box 5700
Bethesda, Maryland 20546
Attention: NASA Representative (5 + 1 Reproducible)

National Aeronautics and Space Administration
Goddard Space Flight Center
Greenbelt, Maryland 20771
Attention: W. R. Cherry
M. Schach
B. Mermelstein, Code 672
J. W. Callaghan, Code 621
Librarian
P. H. Fang, Code 633

National Aeronautics and Space Administration
Lewis Research Center
21000 Brookpark Road
Cleveland, Ohio 44135
Attention: John E. Dilley, M.S. 500-309
B. Lubarsky, M.S. 500-201
H. Shumaker, M.S. 500-201
R. L. Cummings, M.S. 500-201
C. K. Swartz, M.S. 500-201 (3 + 1 Reproducible)
N. D. Sanders, M.S. 302-1
A. E. Potter, M.S. 302-1 (3)
C. S. Corcoran, M.S. 500-201
V. F. Hlavin, M.S. 3-14 (Final Only)
George Mandel, M.S. 5-1 (2)
Report Control Office
Technology Utilization Office, M.S. 3-19
Office of Reliability & Quality Assurance, M.S. 500-203

National Aeronautics & Space Administration
Langley Research Center
Langley Station
Hampton, Virginia 23365
Attention: W. C. Hulton
E. Rind

National Aeronautics & Space Administration
Electronic Research Center
Power Conditioning & Distribution Lab.
575 Technology Square
Cambridge, Massachusetts 02139

Jet Propulsion Laboratory
4800 Oak Grove Drive
Pasadena, California 91103
Attention: John V. Goldsmith
Don W. Ritchie

Institute for Defense Analysis
Connecticut Avenue, N.W.
Washington, D.C. 20546
Attention: R. Hamilton

Advanced Research Projects Agency
Department of Defense, Pentagon
Washington, D.C. 20546
Attention: Dr. C. Yost

Naval Research Laboratory
Department of the Navy
Washington, D.C. 20546
Attention: E. Broncato, Code 6464
M. Wotaw, Code 5170
Dr. V. Linnenbom, Code 7450
Dr. C. Klick, Code 6440

U.S. Army Signal Research and Development Laboratory
Fort Monmouth, New Jersey
Attention: Power Sources Branch

Air Force Cambridge Research Center
Air Research and Development Command
United States Air Force
Laurence G. Hanscom Field
Bedford, Massachusetts
Attention: Col. G. de Giacomo

Air Force Ballistic Missile Division
Air Force Unit Post Office
Los Angeles 45, California
Attention: Col. L. Norman, SSEM
Lt. Col. G. Austin, SSZAS
Lt. Col. A. Bush, SSZME
Capt. A. Johnson, SSZDT
Capt. W. Hoover, SSTRE

Office of the Chief of Engineers
Technical Development Branch
Washington, D.C.
Attention: James E. Melcoln/ENGMC-ED

Aeronautical Research Laboratories
Office of Aerospace Research, USAF
Wright-Patterson Air Force Base
Dayton, Ohio
Attention: Mr. D. C. Reynoles, ARX
Chief, Solid State Physics,
Research Lab.

Aeronautical Systems Division
Air Force Systems Command
United States Air Force
Wright-Patterson Air Force Base, Ohio
Attention: P. R. Betheand
Mrs. E. Tarrants/WWRNEM-1

Flight Vehicle Power Branch
Air Force Aero Propulsion Laboratory
Wright-Patterson Air Force Base, Ohio
Attention: Joe Wise/Code APIP-2

Flight Accessories Aeronautics Systems Division
Wright-Patterson Air Force Base
Dayton, Ohio
Attention: James L. Matice, ASRCM-22

Aerospace Corporation
P.O. Box 95085
Los Angeles 45, California
Attention: Dr. G. Hove
Dr. F. Mozer
V. J. Porfune
Dr. I. Spiro
Technical Library Documents
Group

Battelle Memorial Institute
505 King Avenue
Columbus, Ohio
Attention: L. W. Aukerman
R. E. Bowman
T. Shielladay

Bell and Howell Research Center
360 Sierre Madre Villa
Pasadena, California
Attention: Alan G. Richards

Bell Telephone Laboratories, Incorporated
Murray Hill, New Jersey
Attention: W. L. Brown
U. B. Thomas

Clevite Corporation
Electronic Research Division
540 East 105th Street
Cleveland, Ohio 44108
Attention: Fred A. Shirland
Dr. Hans Jaffe

The Eagle-Picher Company
Chemical and Material Division
Miami Research Laboratories
200 Ninth Avenue, N.E.
Miami, Oklahoma
Attention: John R. Musgrave

Energy Conversion, Incorporated
336 Main Street
Cambridge 42, Massachusetts
Attention: G. J. McCaul

Westinghouse Electric Corporation
Research and Development Laboratories
Churchill Borough, Pennsylvania
Attention: H. G. Chang

Westinghouse Electric Corporation
Semiconductor Division
Youngwood, Pennsylvania
Attention: Don Gunther

Massachusetts Institute of Technology
Security Records Office
Room 14-0641
Cambridge 39, Massachusetts